

PAPER • OPEN ACCESS

## Extracting the differential inverse inelastic mean free path and differential surface excitation probability of Tungsten from X-ray photoelectron spectra and electron energy loss spectra

To cite this article: V P Afanas'ev *et al* 2017 *J. Phys.: Conf. Ser.* **941** 012019

View the [article online](#) for updates and enhancements.

# Extracting the differential inverse inelastic mean free path and differential surface excitation probability of Tungsten from X-ray photoelectron spectra and electron energy loss spectra

V P Afanas'ev<sup>1</sup>, A S Gryazev<sup>1</sup>, D S Efremenko<sup>2</sup>, P S Kaplya<sup>3</sup> and  
A V Kuznetcova<sup>1</sup>

<sup>1</sup> National Research University "Moscow Power Engineering Institute", Department of General Physics and Nuclear Fusion, Krasnokazarmennaya 14, 111250 Moscow, Russia

<sup>2</sup> Deutsches Zentrum für Luft- und Raumfahrt (DLR), Institut für Methodik der Fernerkundung (IMF), 82234 Oberpfaffenhofen, Germany

<sup>3</sup> Raspletina St. 15, 123060 Moscow, Russia

E-mail: GryazevAS@gmail.com

**Abstract.** Precise knowledge of the differential inverse inelastic mean free path (DIIMFP) and differential surface excitation probability (DSEP) of Tungsten is essential for many fields of material science. In this paper, a fitting algorithm is applied for extracting DIIMFP and DSEP from X-ray photoelectron spectra and electron energy loss spectra. The algorithm uses the partial intensity approach as a forward model, in which a spectrum is given as a weighted sum of cross-convolved DIIMFPs and DSEPs. The weights are obtained as solutions of the Riccati and Lyapunov equations derived from the invariant imbedding principle. The inversion algorithm utilizes the parametrization of DIIMFPs and DSEPs on the base of a classical Lorentz oscillator. Unknown parameters of the model are found by using the fitting procedure, which minimizes the residual between measured spectra and forward simulations. It is found that the surface layer of Tungsten contains several sublayers with corresponding Langmuir resonances. The thicknesses of these sublayers are proportional to the periods of corresponding Langmuir oscillations, as predicted by the theory of R.H. Ritchie.

## 1. Introduction

For a long time, Tungsten has attracted interest in material science since it has the highest melting point of all metals, excellent corrosion resistance and low sputtering coefficient. For quantitative studies of energy loss processes of probing electrons, the information on differential inverse inelastic mean free path (DIIMFP) and differential surface excitation probability (DSEP) is required. Several techniques have been proposed for computing DIIMFP and DSEP involving linear response theory and density functional theory. However, such computations are computationally expensive for real atomic structures since a many-body quantum-mechanical problem has to be solved.

An alternative approach to get information on DIIMFP and DSEP is to extract them from electron energy loss spectra [1]. Important results using numerical deconvolution schemes have been given by W. Werner [2] and Afanas'ev et al [3]. However, the DIIMFP and DSEP extraction problem is



severely ill-posed. Consequently, numerical deconvolution procedures can lead to unstable and noisy results containing a set of unphysical peaks in the retrieved functions. Afanas'ev et al [4] proposed a so-called fitting approach, in which the desired functions are parametrized on the base of a classical Lorentz oscillator. Unknown parameters are found by using the fitting procedure, which consists of computing the simulated spectra in a given energy loss range and matching them with the corresponding measurements. This method has been successfully applied for extracting inelastic scattering parameters of Be, Mg, Al, Si and Nb. The intent of this paper is to retrieve DIIMFP and DSEP for Tungsten from X-ray photoelectron spectra (PES) and transmission electron energy loss spectra (TEELS) using the fitting approach.

## 2. Methodology

### 2.1. Forward model: simulating PES and TEELS spectra

The forward model is used for computations of PES and TEELS. It is based on the partial intensity approach [5], in which a spectrum is given as a weighted sum of the cross-convolved DIIMFP and DSEP. The weights can be found by using either the Monte-Carlo method, or the invariant imbedding method. In the latter case, a set of the matrix Riccati and Lyapunov equations is derived and solved numerically by using the backward differential formula (BDF). The computational details are described in [6] and references therein. Both PES and TEELS are computed within the same framework. Note that this procedure rigorously accounts for multiple scattering processes (unlike, e.g.,  $P_1$ - and the transport approximations) and computationally efficient. For instance, it requires less than 0.01 seconds for computing one PES spectrum on Intel Xeon CPU E5-1620 3.60 GHz. Hence, the forward model performance is not an issue in the retrieval procedure.

### 2.2. Modeling of inelastic scattering properties

The physics of inelastic energy losses in solids is well-known. It involves excitation of collective Langmuir oscillations of free electrons and local ionization processes. At the sample interface, there is a different loss mode due to a surface plasmon with frequency approximately by a factor  $\sqrt{2}$  lower than that of the bulk plasmon. The surface excitations are taken into account by introducing an additional layer at the interface, in which the inelastic energy loss is described by DSEP. For transition metals, the situation is more complicated since two surface plasmons can be detected in high energy resolution spectra (e.g., see [4, 7] for Niobium studies). Consequently, a finer spatial discretization of inelastic scattering properties may be required, and the surface layer is divided into two sublayers. In this paper, the model with the following peculiarities is used:

- the sample is assumed to have three layers, namely, surface (S), transitional (G) and bulk (B); using this nomenclature, DIIMFP is related to the bulk, while DSEP is used for S- and G-layers;
- each layer contains a plasmon with a corresponding frequency  $\omega = 2\pi/T$ , where  $T$  is the period of oscillations. In the energy loss spectrum, these plasmons form two peaks centered at energies  $\hbar\omega_S$  and  $\hbar\omega_G$  with  $\hbar$  the reduced Planck constant;
- following Ritchie [8], the thicknesses of S- and G- sublayers are given as

$$d_S = T_S v_e, \quad d_G = T_G v_e, \quad (1)$$

where  $T_S$  and  $T_G$  are the periods of oscillations in S- and G-sublayers, respectively, and  $v_e$  is the electron velocity.

Bearing this in mind, the unknown DIIMFP and DSEPs are sought using the following ansatz:

$$x_{\text{in}}(\Delta) = \left[ \sum_{i=1}^{N_{\text{pl}}} \lambda_{\text{pl } i} x_{\text{pl } i}(\Delta) + \sum_{j=1}^{N_{\text{ion}}} \lambda_{\text{ion } j} x_{\text{ion } j}(\Delta) \right]. \quad (2)$$

Here  $N_{pl}$  and  $N_{ion}$  are the numbers of plasmon and ionization processes taken into account, respectively,  $\lambda_{pl}$  and  $\lambda_{ion}$  are the corresponding weights, while  $x_{pl}(\Delta)$  and  $x_{ion}(\Delta)$  are the basic functions for the plasmon and ionization processes, respectively. For  $x_{pl}(\Delta)$  the following representation is used

$$x_{pl i}(\Delta) = A_{pl i} \frac{\Delta^\beta}{(\Delta^2 - \varepsilon_{pl i}^2)^2 + \Delta^\alpha b_i^{4-\alpha}}. \quad (3)$$

Here,  $A_{pl}$  is the normalization coefficient,  $\varepsilon_{pl}$  is the effective plasmon energy related to the plasmon peak position,  $b$  is the attenuation coefficient which governs the plasmon peak width, while  $\alpha$  and  $\beta$  are the tuning parameters which control the peak asymmetry and enhance the fitting. Essentially, Eq. (2) is a modification of the dispersion relation in solids and generalizes the excitation function of a classical Lorentz oscillator. The energy losses for ionization are described in the frameworks of classical Thompson theory [9]

$$x_{ion j}(\Delta) = \frac{A_{ion j}}{\Delta^{2+a_j}} \eta(\Delta - J_{ion j}), \quad (4)$$

with  $A_{ion j}$  the normalization coefficient,  $\eta$  the Heaviside step function,  $J_{ion j}$  the ionization potential, and  $a$  the coefficient accounting for the electron screening of a Coulomb potential. Finally, for  $\lambda_{pl}$  and  $\lambda_{ion}$  the following normalization condition is used

$$\sum_{i=1}^{N_{pl}} \lambda_{pl i} + \sum_{j=1}^{N_{ion}} \lambda_{ion j} = 1. \quad (5)$$

Unknown parameters of the model are found by using the fitting procedure, which minimizes the residual between the forward model simulations and corresponding measurements. The constraints (1) and (5) are explicitly implied in the retrieval algorithm.

### 3. Results and discussion

For DIIMFP and DSEP retrieval we take PES and TEELS data from [10] and [11], respectively. Figure 1 shows the PES data. The photoelectron spectrum was induced by  $K_\alpha$  line of Al corresponding to 1486.6 eV. The spectrum can be regarded as a superposition of several spectra induced by the photoelectron emission from levels  $4f_{7/2}$ ,  $4f_{5/2}$ ,  $5p_{3/2}$ ,  $5p_{1/2}$ ,  $5s_{1/2}$ . Such overlapping hinders the fine structure of the spectrum. Consequently, only one surface Plasmon can be observed in the PES. Therefore, here the two-layer model is used [3, 12]. The DIIMFP and DSEP are retrieved in the energy range 1360–1460 eV.

The high resolution TEELS data is shown in Figure 2. The measurements have been performed along the probe direction providing high intensity of the signal. Besides the bulk plasmon at energy  $\hbar\omega_B = 24.0$  eV, two surface plasmons are observed at energies  $\hbar\omega_S = 10.4$  eV,  $\hbar\omega_G = 15.6$  eV. Hence, two DSEPs, namely,  $x_{inS}(\Delta)$  and  $x_{inG}(\Delta)$ , should be used for the TEELS data interpretation.

Retrieved DIIMFPs and DSEPs within the two-layer model from PES data and the three-layer model from TEELS data are shown in Figure 3. The extracted functions are compared against data from W.S.M. Werner [13] obtained assuming homogeneous inelastic scattering properties throughout the sample. Table 1 lists the values of the fitted parameters. From Figure 3, it can be seen that the one-layer model can predict the energies of plasmons and ionization potentials. However, it fails to correctly reproduce the shape of DIIMFPs. Instead, it provides an effective DIIMFP being some kind of mixture of the actual DIIMFP, DSEP and their cross-convolutions. The functions retrieved from PES data agree well with those from TEELS.

Fitted PES and TEELS computed using retrieved DIIMFP/DSEPs are shown in Figures 1 and 2, respectively. The simulated spectra are in good agreement with experimental results. Note, that both EELS and PES data are interpreted within the same physical model for inelastic scattering energy losses without accounting intrinsic excitations [14].

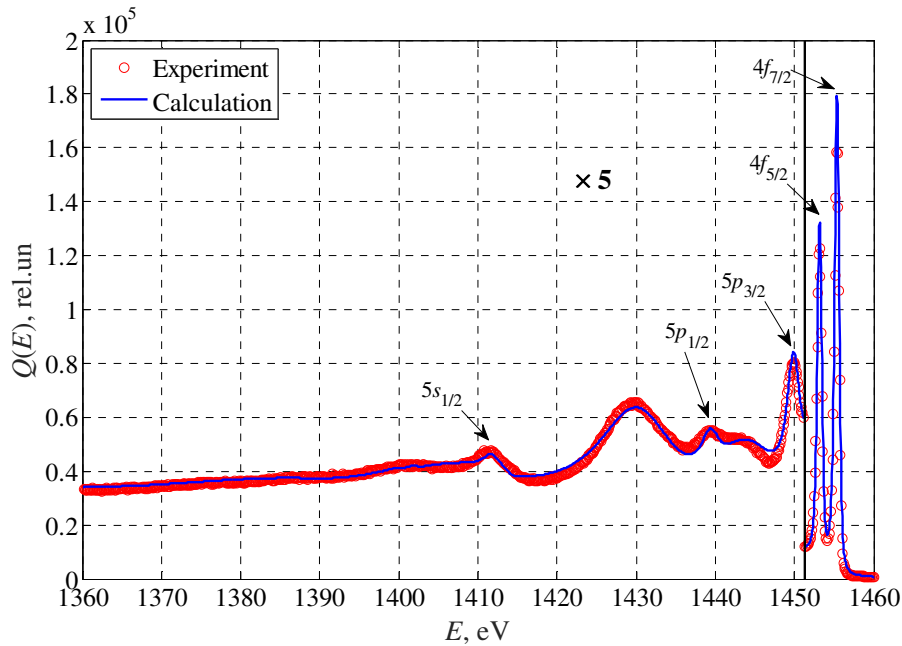


**Figure 1.** PES data of Tungsten. X-ray probing by monochromatic emission of line  $\text{Al K}\alpha$ . Experimental data is taken from [10]. The circles refer to measurements, while the solid line corresponds to the computed spectrum using retrieved DIIMFP and DSEP functions.

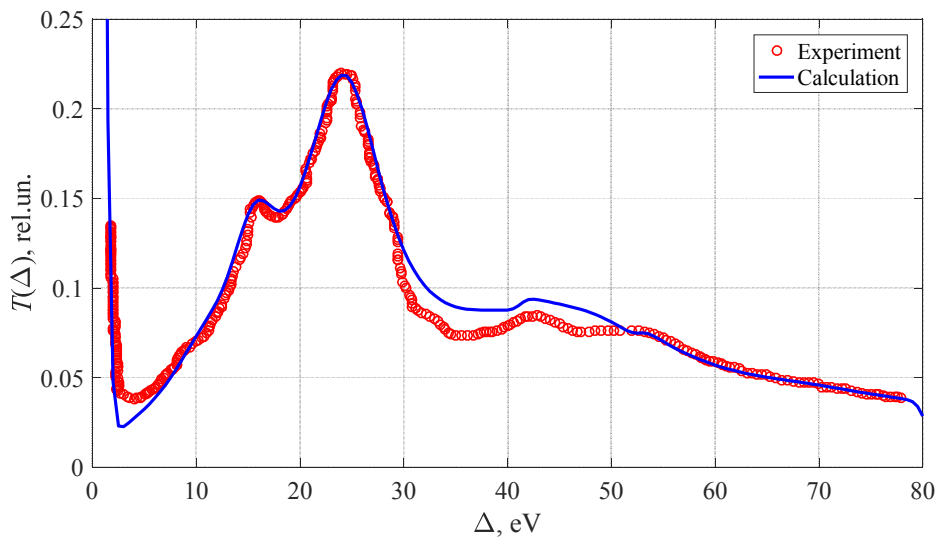


**Figure 2.** TEELS spectrum of the Tungsten foil. The thickness of the foil is about 30 nm. The incident electron energy is 25 keV. Sighting is in the probe direction. Measurements are taken from [11]. DIIMFP  $x_m(\Delta)$  is extracted using the three-layer model.

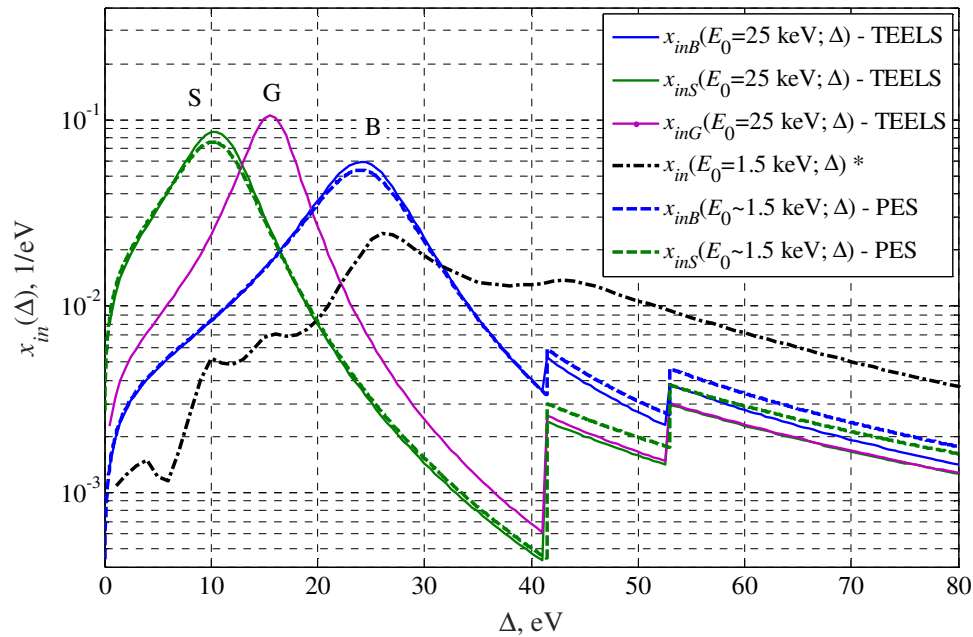


**Figure 3.** Extracted DIIMFP for bulk  $x_{inB}(\Delta)$  and DSEPs for surface layers  $x_{inG}(\Delta)$  and  $x_{inS}(\Delta)$ .  
\* Dash-and-dot line corresponds to the data from [13].

**Table 1.** Retrieved DIIMFP and DSEPs parameters for Tungsten and thicknesses of layers.

Parameter	from TEELS spectrum, $E_0=25$ keV			from PES spectrum, $E_0\sim 1.5$ keV	
	B-layer	G-layer	S-layer	B-layer	S-layer
$\epsilon_{pl}$	24.6	15.8	11.0	24.6	11.0
$b$	11.9	6.8	8	12.5	8.7
$\alpha$		1.5			0.5
$\beta$		0.5			0.5
$J_{ion1}$		41.5			41.5
$\lambda_{ion1}$		0.10			0.13
$J_{ion2}$		53			53
$\lambda_{ion2}$		0.10			0.13
$d$ , nm	21.0	2-2.5	2-1.0	$\infty$	0.68

#### 4. Summary

The fitting approach has been applied to PES and TEELS data to retrieve DIIMFP and DSEP functions of Tungsten. It has been shown that for high-energy resolution TEELS data, it is mandatory to account for two surface plasmons at the interface, while for low resolution PES data it is sufficient to consider only one surface plasmon. The parametrization of DIIMFP/DSEP functions using the classical Lorentz oscillator expressions can be regarded as a regularization procedure, which guarantees a physically consistent result.

The fitting approach for extracting inelastic scattering properties is applicable to the hydrogen depth profiling [15, 16] using the elastic peak electron spectroscopy [17]. There, the DIIMFP overlaps the hydrogen peak and introduces a systematic error in the retrieved hydrogen concentration. The

method described in this paper is suitable for designing an inelastic scattering background subtraction tool. This is a topic for our future research.

### Acknowledgments

This work has been supported by the grant of the Russian Science Foundation (project No. 16-19-10027).

### References

- [1] Tougaard S, Chorkendorff I 1987 *Phys. Rev. B* **35** 6570
- [2] Werner W S M 2006 *Appl. Phys. Lett.* **89** 213106
- [3] Afanas'ev V P, Efremenko D S, Lubenchenko A V 2011 *J. Surf. Invest.* **5**(2) 375
- [4] Afanas'ev V P, Gryazev A S, Efremenko D S, Kaplya P S 2017 *Vacuum* **136** 146
- [5] Werner W S M 1995 *Surface Interface Analysis* **23** 737
- [6] Afanas'ev V P, Efremenko D S, Kaplya P S 2016 *J. Electron Spectrosc. Relat. Phenom.* **210** 16
- [7] Afanasyev V P, Efremenko D S, Lubenchenko A V, Vos M, Went M R 2010 *Bull. Russian Acad. Sci.: Physics* **72** (2) 170
- [8] Ritchie R H 1957 *Phys. Rev.* **106** 874
- [9] Radzig A A, Smirnov B M 1985 *Reference Data on Atoms, Molecules, and Ions* (Springer Series in Chemical Physics vol 31) ed J P Toennies (Berlin, Heidelberg: SpringerBerlin Heidelberg)
- [10] Moulder J, Stickle W, Sobol P, Bomben K 1995 *Handbook of X-Ray Photoelectron Spectroscopy* (Eden Prairie, Minnesota: Perkin-Elmer Corporation, Physical Electronics Division)
- [11] Zharnikov M V, Gorobchenko V D, Serpuchenko I L 1987 *JETP* **65** (1) 128
- [12] Afanas'ev V P, Golovina O Y, Gryazev A S, Efremenko D S, Kaplya P S 2015 *J. Vac. Sci. Technol. B* **33** (3) 03D101
- [13] Werner W S M, Glantschnig K, Ambrosch-Draxl C 2009 *J. Phys. Chem. Ref. Data.* **38** 1013
- [14] Yubero F, Tougaard S 2005 *Phys. Rev. B.* **71** 045414
- [15] Kostanovskiy I A, Afanas'ev V P, Naujoks D, Mayer M 2015 *J. Electron Spectrosc. Relat. Phenom.* **202** 22
- [16] Afanas'ev V P, Gryazev A S, Efremenko D S, Kaplya P S, Ridzel O Y 2016 *J. Phys. Conf. Ser.* **748** 012005
- [17] Vos M, Went M R 2009 *J. Phys. B: At. Mol. Opt. Phys.* **42** 065204